ELSEVIER

Thermochimica Acta 256 (1995) 339–346

thermochimica acta

Thermal decomposition of iron(III) oxalate–magnesium oxalate mixtures

S.N. Basahel [a], A.A. El-Bellihi [b], M. Gabal [b], El-H.M. Diefallah [a,*]

[a] *Department of Chemistry, Faculty of Science, King Abdulaziz University, Jeddah, Saudi Arabia*
[b] *Department of Chemistry, Faculty of Science, Benha, Egypt*

Received 26 July 1994; accepted 25 October 1994

Abstract

The differential thermal analysis–thermogravimetry (DTA–TG) behaviour of chemically coprecipitated iron(III) oxalate–magnesium oxalate (1 : 1 mole ratio) was investigated. X-ray diffractometry (XRD) of samples calcined at different temperatures showed that magnesium ferrite is formed in samples heated at higher temperatures. Integral composite analyses of dynamic TG data of the decomposition reactions in the coprecipitated mixture were carried out using various solid state reaction model equations, and the results showed that the decomposition reactions are best described by the two- and three-phase boundary, R_2 and R_3 models. Kinetic analyses of dynamic data were also carried out in accordance with the integral methods of Ozawa and Coats–Redfern and the results are discussed in comparison with the integral composite analysis of data.

Keywords: Decomposition; DTA; Iron oxalate; Magnesium oxalate; Oxalate; TG; XRD

1. Introduction

The thermal decomposition of metal oxalates has been the subject of numerous investigations. The behaviour of the thermal decomposition and the stability of salts of simple metal oxalates have been reviewed [1]. Dollimore [2] has also discussed the thermodynamic, kinetic and textural features of metal formation of

* Corresponding author.

SSDI 0040-6031(94)02158-9

the decomposition of oxysalts. The thermal decomposition behaviour and the chemical composition and physical properties of the end products are determined by the ambient atmosphere, the rate of heating, sample weight and final temperature of heating. Quite often the thermal decomposition of such materials results in a product, e.g. oxide or metal, which possesses pores, lattice imperfections and other characteristics that are necessary for its function as a reactive solid; some oxalates have been considered as economic catalyst precursors [3]. There has been increasing interest in studying the experimental factors and processing parameters, especially in determining the kinetics of the thermal decomposition reactions of oxysalts [4,5].

The thermal decomposition of ferrous oxalate [6–10], ferric oxalate [8–10] and the oxalato complexes of iron [10,11] were studied in air and N_2 atmospheres using DTA–TG, X-ray diffraction and Mössbauer effects techniques. In studying the thermal decomposition of anhydrous magnesium and zinc oxalates [12], it was concluded that the energy barrier to reaction is not diminished by the product oxide and that the reaction is controlled by an electron-transfer step. In the present study, DTA–TG techniques were used to study the thermal decomposition reactions in chemically coprecipitated ferric oxalate–magnesium oxalate (1 : 1 mole ratio) and the XRD technique was used to examine samples calcined at different temperatures. Kinetic analyses of non-isothermal results of the decomposition reactions in the mixture were carried out using various solid state reaction model equations and integral methods of dynamic data analysis.

2. Experimental

Iron(III) oxalate–magnesium oxalate was precipitated by the addition of aqueous oxalic acid solution to a hot, vigorously stirred, aqueous solution of AnalaR iron and magnesium nitrates with a mole ratio of 2 : 1. The coprecipitated oxalate mixture was digested on a water bath for about 1 h, filtered, washed with chilled water and then with acetone, air dried, and then kept in a desiccator.

Simultaneous DTA–TG curves were obtained using a Shimadzu model 40 thermal analyser. Experiments were carried out in air against α-alumina as a reference, at heating rates of 5, 10, 15 and 20°C min^{-1}. XRD patterns for the calcined mixtures of 1 : 1 mole ratio were recorded using a Shimadzu X-ray diffraction unit, with Cu target and Ni filter.

3. Results and discussion

Fig. 1 shows DTA–TG traces of the coprecipitated mixture $MgC_2O_4 \cdot 2H_2O$–$Fe_2(C_2O_4)_3 \cdot 6H_2O$ in air. The TG curve shows three steps. The first step corresponds to complete dehydration and decomposition of Fe(III) oxalate to Fe(II) oxalate and is associated with two peaks in the DTA, one endo (at 110°C) due to dehydration, and one sharp exo (at 180°C) associated with the decomposition. The

second step in the TG immediately follows the first step, with an inflexion point but no plateau, over which the anhydrous Fe(II) oxalate is stable, and corresponding to the decomposition and oxidation of FeC_2O_4. This second step is associated with two exo effects in the DTA, one large peak (at 220°C) and a small peak at about 340°C. The third step in the TG corresponds to the decomposition of MgC_2O_4 and formation of MgO and is associated with one exo effect in the DTA trace (peak at 420°C).

X-ray diffraction patterns (Fig. 2) show that the decomposition to oxides (MgO and Fe_2O_3) precedes the formation of magnesium ferrite by more then 200°C. The XRD patterns were obtained for the starting material and for samples heated for 5 min at 100, 200, 400, 600, 700 and 800°C in air. The starting material gave an XRD pattern which generally agrees with the results reported in the ASTM data cards for the hydrated oxalates of iron(III) and Mg. At 100°C, the XRD patterns show low-intensity lines of the anhydrous salts due to partial dehydration of the sample. At 200°C, dehydration is complete and lines due to FeC_2O_4 are apparent. Samples heated between 300 and 600°C show XRD patterns characteristic of MgO and Fe_2O_3. At 700°C and above, diffraction lines of magnesium ferrite are prominent.

Fig. 3 shows the dynamic TG measurements of the three decomposition steps of the coprecipitated mixture $MgC_2O_4 \cdot 2H_2O$–$Fe^2(C_2O_4)_3 \cdot 6H_2O$. Kinetic analyses of the non-isothermal TG curves were carried out using three approximate integral methods, the Ozawa [13], Coats–Redfern [14] and Diefallah [5]. Under non-isother-

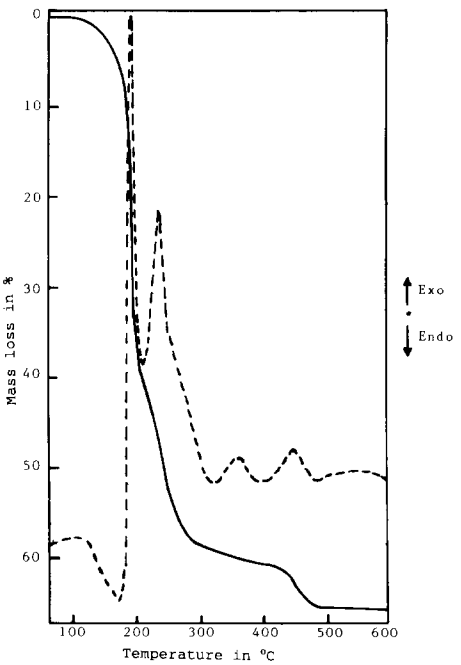

Fig. 1. DTA–TG curves of 1 : 1 mole ratio coprecipitated magnesium oxalate–iron(III) oxalate hydrated mixture in air. Heating rate 30°C min^{-1}.

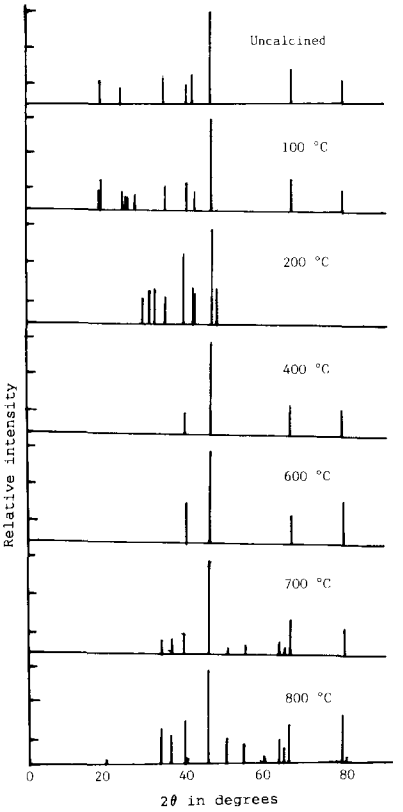

Fig. 2. X-ray diffraction patterns of samples of $MgC_2O_4 \cdot 2H_2O$–$Fe_2(C_2O_4)_3 \cdot 6H_2O$ (1 : 1 mole ratio) calcined at the specified temperatures.

mal conditions and with the heating rate set to a constant value β, the kinetic model function $g(\alpha)$ is given by the Doyle equation [15]

$$g(\alpha) = \frac{A}{\beta} \int_0^T \exp\left(-\frac{E}{RT}\right) dT = \frac{AE}{R\beta} P(x)$$

The function $P(x)$ has been defined as

$$P(x) = \frac{e^{-x}}{x} - \int_0^{x_0} \frac{e^{u}}{u} du$$

where $u = E/(RT)$ and x is the corresponding value of u at which a fraction α of a material has decomposed.

In the Coats–Redfern method [14], the function $g(\alpha)$ is approximated to the form

$$g(\alpha) = \frac{ART^2}{\beta E}\left[1 - \frac{2RT}{E}\right] e^{-E/RT}$$

The equation has been written in the form

$$-\ln\left[\frac{g(\alpha)}{T^2}\right] = -\ln\frac{AR}{\beta E}\left(1-\frac{2RT}{E}\right)+\frac{E}{RT}$$

The quantity $\ln\{(AR/\beta E)[1-(2RT/E)]\}$ is resonably constant for most values of E and in the temperature range over which most reactions occur.

In the Ozawa method [13], a master curve is derived from the TG data obtained at different heating rates (β) using the Doyle equation and assuming that $\{(AE/R\beta)[P(E/RT)]\}$ is a constant for a given function of material decomposed. The function $P(E/RT)$ is approximated by the equation

$$\log P\left(\frac{E}{RT}\right) = -2.315-0.4567\left(\frac{E}{RT}\right)$$

so that

$$-\log\beta = 0.4567\left(\frac{E}{RT}\right)+\text{constant}$$

Hence, the activation energy is calculated from the thermogravimetric data obtained at different heating rates. The frequency factor is calculated from the equation

$$\log A = \log g(\alpha)-\log\left[\frac{E}{\beta R}P\left(\frac{E}{RT}\right)\right]$$

It is obvious that the calculation of E is independent of the reaction model used to describe the reaction, whereas the frequency factor depends on the determined form of $g(\alpha)$.

In the composite method of analysis of dynamic data [5,16], the results obtained not only at different heating rates, but also with different α values, are superimposed on one master curve. This can be achieved either by use of the modified

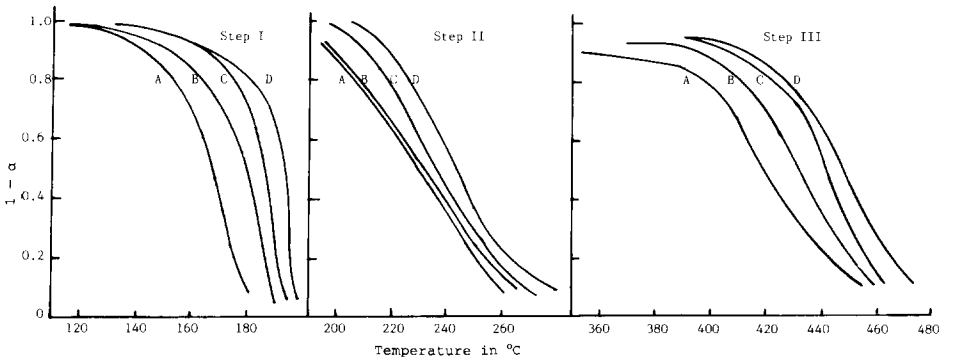

Fig. 3. Dynamic measurements of the thermal decomposition steps of 1 : 1 mole ratio coprecipitated $MgC_2O_4\cdot 2H_2O$–$Fe_2(C_2O_4)_3\cdot 6H_2O$ mixtures. Heating rate: curve A, 5°C min^{-1}; curve B, 10°C min^{-1}; curve C, 15°C min^{-1}; curve D, 30°C min^{-1}.

Coats–Redfern equation [17] (composite I) or the Doyle equation [15] (composite II). In general the results show that both composite methods of analysis gave equivalent curves and identical values for the activation parameters [5,16].

In composite method I, the modified Coats–Redfern equation is written in the form

$$\ln\left[\frac{\beta g(\alpha)}{T^2}\right] = \ln\left(\frac{AR}{E}\right) - \frac{E}{RT}$$

Hence, the dependence of $\ln[\beta g(\alpha)/T^2]$, calculated for different α values at their respective β values, on $1/T$ must give rise to a single master straight line for the correct form of $g(\alpha)$ and a single activation energy and frequency factor can readily be calculated.

In composite method II, the Doyle equation is rewritten in the form

$$\log g(\alpha)\beta = \left[\log\frac{AE}{R} - 2.315\right] - 0.4567\frac{E}{RT}$$

Again, the dependence of $\log g(\alpha)\beta$, calculated for the different α values at their respective β values, on $1/T$ must give rise to a single master straight line for the correct form of $g(\alpha)$.

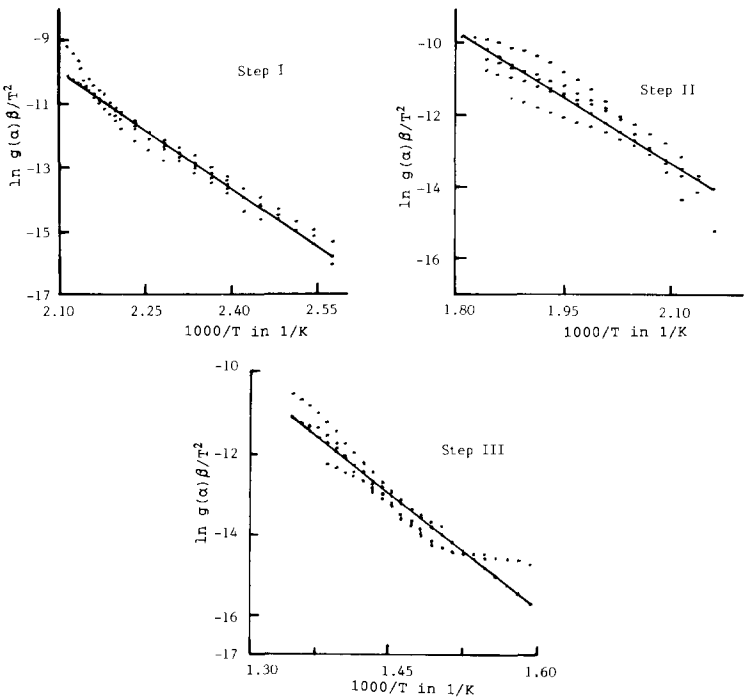

Fig. 4. Integral analysis of dynamic TG data of the three decomposition steps based on the modified Coats–Redfern equation (composite I), assuming R_3 model.

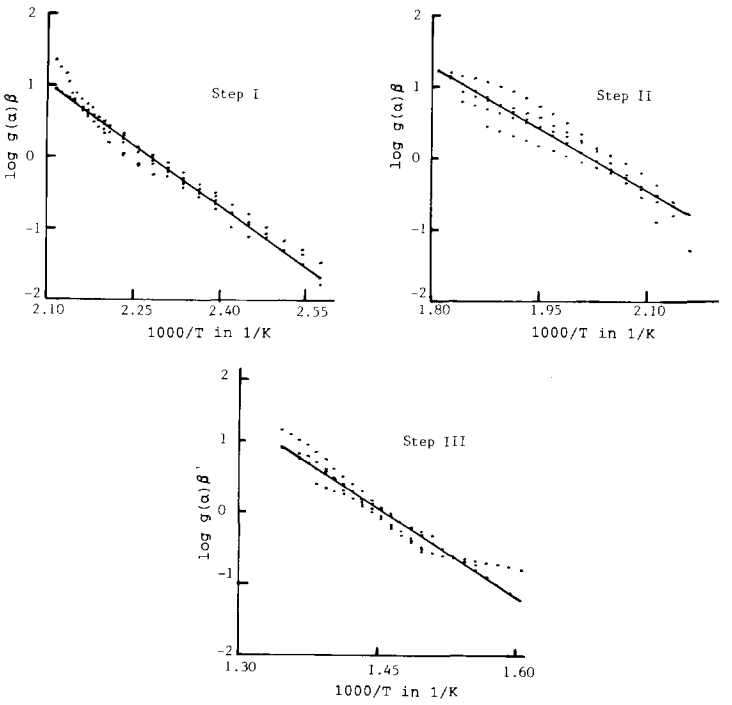

Fig. 5. Integral analysis of dynamic TG data of the three decomposition steps based on the Doyle equation (composite II), assuming R_3 model.

The integral composite analysis of dynamic TG data of the three decomposition steps, when carried out using the various solid state reaction models [4,5], showed that the decomposition reactions are best described by the two- and three-dimensional phase boundary, R_2 and R_3 models, respectively. Figs. 4 and 5 show the results of the composite analysis of dynamic TG data with respect to the R_3 model.

The activation energies and frequency factors of the three decomposition steps were calculated by linear regression using the three integral methods of kinetic data analysis and assuming R_3 function. The results, listed in Table 1, show that the Coats–Redfern and the composite methods are in good agreement, with the composite methods showing least deviation, but the results of the Ozawa method are not in agreement and show large deviations. In general, the first and second decomposition steps have comparable activation energies and frequency factors, whereas the activation energy of the third step is higher by about 50%.

The decomposition of a metal oxalate occurs when a temperature is reached at which rupture of the M–O bond is possible or at which rupture of the C–O bond occurs [18]. It is noted (Table 1) that MgC_2O_4 decomposition (step III) requires a higher activation energy (about 50% more according to the Coats–Redfern and composite methods of analysis) than the FeC_2O_4 decomposition (step II). The radius of Mg^{2+} (0.65 Å) is smaller than that of Fe^{2+} (0.76 Å) and based on

Table 1
Activation parameters of the three thermal decomposition steps of coprecipitated $MgC_2O_4 \cdot 2H_2O$–$Fe_2(C_2O_4)_3 \cdot 6H_2O$ mixtures (1 : 1 mole ratio) calculated according to the R_3 model

Method of analysis	Step I		Step II		Step III	
	E_i (kJ mol^{-1})	log i (A min^{-1})	E_i (kJ mol^{-1})	log i (A min^{-1})	E_i (kJ mol^{-1})	log i (A min^{-1})
Coats-Redfern	104 ± 8	11.2 ± 1	92 ± 13	8.4 ± 1.4	157 ± 38	10.5 ± 3.1
Ozawa	115 ± 26	12.7 ± 3.2	225 ± 70	22 ± 7	242 ± 77	16.8 ± 6
Composite I	101 ± 2	10.9 ± 0.6	102 ± 5	9.5 ± 1.3	147 ± 5	9.7 ± 0.9
Composite II	103 ± 2	10.1 ± 0.3	105 ± 5	9.9 ± 0.6	150 ± 5	10.1 ± 0.4

coulombic attraction, the Mg^{2+} ions will have a stronger M–O bond than the Fe^{2+} ion. This would increase the energy needed to break the Mg–O bond and liberate CO_2, and thus increases the activation energy for the reaction.

References

[1] D. Dollimore, Thermochim. Acta, 117 (1987) 331.
[2] D. Dollimore, Thermochim. Acta, 177 (1991) 59.
[3] V.V. Boldyrev, M. Bulens and B. Delman, The Control of the Reactivity of Solids, Elsevier, Amsterdam, 1979.
[4] M.E. Brown, D. Dollimore and A.K. Galwey, in C.H. Bamford and C.F.H. Tipper (Eds.), Comprehensive Chemical Kinetics, Vol. 22, Elsevier, Amsterdam, 1980, p. 218.
[5] El-H.M. Diefallah, Thermochim. Acta, 202 (1992) 1.
[6] B. Boyanov, D. Khadzhiev and V. Vasilev-Plovdiv, Thermochim. Acta, 93 (1985) 1968.
[7] U. Kozo, J. Chem. Soc. Jpn., 6 (1975) 1968.
[8] P.K. Gallagher and C.R. Kurkjian, Inorg. Chem., 5 (1966) 214.
[9] D. Dollimore and N. Nicholson, J. Chem. Soc. A, (1966) 281.
[10] D. Broadbent, D. Dollimore and J. Dollimore, J. Chem. Soc. A, (1967) 451.
[11] J.D. Danforth and J. Dix, Inorg. Chem., 10 (1971) 1623.
[12] J.D. Danforth and J. Dix, J. Am. Chem. Soc., 93 (1971) 6843.
[13] T. Ozawa, Bull. Chem. Soc. Jpn., 38 (1965) 1881; J. Therm. Anal., 2 (1970) 301.
[14] A.W. Coats and J.P. Redfern, Nature, 201 (1964) 68.
[15] C.D. Doyle, J. Appl. Polym. Sci., 5 (1961) 285.
[16] S.N. Basahel, A.A. El-Bellihi and El-H.M. Diefallah, J. Therm. Anal., 39 (1993) 87.
El-H.M. Diefallah, A.A. El-Bellihi, S.N. Basahel, M. Abdel Wahab and Z.A. Omran, Thermochim. Acta, 230 (1993) 143.
S.N. Basahel, M.M. El-Fass, A.A. El-Bellihi, E.A. Al-Sabban and El-H.M. Diefallah, Radiat. Phys. Chem., in press (1994).
[17] J.M. Criado, Thermochim. Acta, 24 (1978) 186.
[18] D. Dollimore, D.L. Griffiths and D. Nicholson, J. Chem. Soc., (1963) 2617.